Physical, mechanical and thermal behavior of concrete block stabilized with glass fiber reinforced polymer waste

Comportamento físico, mecânico e térmico do bloco de concreto estabilizado com resíduo de polímero reforçado com fibra de vidro

Comportamiento físico, mecánico y térmico del bloque de hormigón estabilizado con residuos de polímero reforzado con fibra de vidrio

Jaqueline Damiany Portela
ORCID: https://orcid.org/0000-0003-3944-3928
Universidade Federal de Lavras, Brasil
E-mail: jaqueline-portela@outlook.com

Rômulo Marçal Gandia
ORCID: https://orcid.org/0000-0002-7786-1525
Universidade Federal de Lavras, Brasil
E-mail: romagandia@gmail.com

Bárbara Lemes Outeiro Araújo
ORCID: https://orcid.org/0000-0001-5350-5174
Universidade Federal de Lavras, Brasil
E-mail: barbara@oleo.ufla.br

Rodrigo Allan Pereira
ORCID: https://orcid.org/0000-0002-1628-1172
Universidade Federal de Lavras, Brasil
E-mail: rodrigo.apereira@deg.ufla.br

Francisco Carlos Gomes
ORCID: https://orcid.org/0000-0002-4957-094X
Universidade Federal de Lavras, Brasil
E-mail: fcgomes@ufla.br

Abstract

The Glass Fiber Reinforced Polymer (GFRP) waste despite having excellent physical and mechanical properties is still largely unexplored besides presenting large volume of waste

with very low degradability. The use of concrete block presents high resistance to compression, low price high masonry coating ratio by material weight, however high thermal conductivity. Therefore, the study aimed to produce and investigate the effect of adding GRFP residues to concrete blocks due to physical, mechanical and thermal properties. The compositions were made by replacing the fine gravel between 0 to 10% in mass by the GFRP residue. They were evaluated from physical, mechanical and thermal tests. The results showed that the use of GFRP residue did not interfere in water absorption and compressive strength, despite the significant increase in mechanical energy absorption of the material. Thermal conductivity reduced by 46% and the concrete blocks were 7% lighter. In addition to providing a destination for a considerable quantity of the waste, the commercial value of the final product is higher due to using a residue with low degradability and high energy power due to burning during recycling.

Keywords: Construction materials; Sustainability; Residue; Thermal conductivity; GFRP waste.

Resumo

O resíduo de Polímero Reforçado com Fibra de Vidro (PRFV) apesar de possuir excelentes propriedades físicas e mecânicas ainda é pouco explorado além de apresentar grande volume de resíduo com baixíssima degradabilidade. O uso de bloco de concreto tem alta resistência à compressão, baixo preço e elevada relação do revestimento de alvenaria pelo peso do material, porém alta condutividade térmica. Portanto, este trabalho foi realizado objetivando-se utilizar os resíduos da PRFV na produção de blocos de concreto. As composições foram feitas substituindo o cascalho fino entre 0 a 10% em massa pelo resíduo de PRFV. Eles foram avaliados a partir de testes físicos, mecânicos e térmicos. Os resultados mostraram que a utilização do resíduo de PRFV não interferiu na absorção de água e na resistência à compressão, apesar do aumento significativo na absorção de energia mecânica do material. A condutividade térmica foi reduzida em 46% e os blocos de concreto ficaram 7% mais leves. Além de dar destinação a uma quantidade considerável de resíduos, o valor comercial do produto final é maior devido à utilização de um resíduo de baixa degradabilidade e alto poder energético devido à queima durante a reciclagem.

Palavras-chave: Materiais de construção; Sustentabilidade; Resíduo; Condutividade térmica; Resíduo PRFV.

Resumen

Los residuos de polímero reforzado con fibra de vidrio (GFRP), a pesar de tener excelentes propiedades físicas y mecánicas, aún están en gran parte inexplorados, además de presentar un gran volumen de residuos con muy baja degradabilidad. El uso de bloques de hormigón presenta alta resistencia a la compresión, bajo precio, alta relación de revestimiento de mampostería por peso del material, sin embargo alta conductividad térmica. Por lo tanto, el objetivo de este trabajo era utilizar los residuos de PRFV en la producción de bloques de hormigón. Las composiciones se prepararon reemplazando la grava fina entre el 0 y el 10% en masa por el residuo de GFRP. Fueron evaluados a partir de pruebas físicas, mecánicas y térmicas. Los resultados mostraron que el uso de residuos de GFRP no interfirió en la absorción de agua y la resistencia a la compresión, a pesar del aumento significativo en la absorción de energía mecánica del material. La conductividad térmica se redujo en un 46% y los bloques de hormigón fueron un 7% más ligeros. Además de proporcionar un destino para una cantidad considerable de residuos, el valor comercial del producto final es mayor debido al uso de un residuo de baja degradabilidad y alto poder energético debido a la quema durante el reciclaje.

Palabras clave: Materiales de construcción; Sostenibilidad; Residuo; Conductividad térmica; Residuos de PRFV.

1. Introduction

The concrete block has several advantages over ceramic building materials, such as economic viability, standardized materials, ease of production and lower energy expenditure (Gandia, Campos, Corrêa, & Gomes, 2018).

One of the biggest challenges of the concrete block is the thermal comfort provided by the thermal conductivity of the material. The concrete block has relatively high thermal conductivity, resulting in thermal discomfort and increasing the cost of cooling / heating. Authors have been proposing the use of various materials combined with cement matrix trying to solve this challenge (Alyousef, Benjeddou, Soussi, Khadimallah, & Jedidi, 2019; Callejas, Durante, & Oliveira, 2017; Dimitrioglou et al., 2016; Fajardo, Torres, & Moreno, 2015; Kanchanapiya, Methacanon, & Tantisattayakul, 2018; Kus, Özkan, Göcer, & Edis 2013; Udawattha & Halwatura, 2018; Xu, Chen, Zhang, Gao, & Huang, 2016; Zaetang, Sata, Wongsa, & Chindaprasirt, 2016; Zhu, Dai, Bai, & Zhang, 2015).

The energy concern and the large generation of low degradability residues are proposed several studies aiming the use of residues in building materials, since the construction sector is the one that demands the most energy in a world scale. Partial replacement of aggregates by synthetic and natural residues in cement-based building materials is a target of research.

Research demonstrating the improvement in cement matrices using fibers are recent (Shuh-Huei, Shah, Zongjin, & Toshio, 1993; Soroushian & Bayasi, 1991; Swamy 1975). The Incorporation of wastes, fibers and other stabilizers such as: PET bottles, recycled demolition aggregate, glasses of different origins and sizes, wood fiber waste, rice rusk ash, limestone powder waste, ceramic brik residues, carbon nanotube, sewage sludge ash, polypropylene fibres, cotton waste and other wastes and stabilizers in cementitious building materials demonstrate stability or advances related to physical, mechanical and thermal properties (Algin & Turgut, 2008; Ascione, De Felice, & De Santis, 2015; Bilodeau, Kodur, & Hoff, 2004; Brandt, 2008; Carozzi, Milani, & Poggi, 2014; Chen, Li, & Poon, 2018; Choi, Moon, Chung, & Cho, 2005; Konsta-Gdoutos, Metaxa, & Shah, 2010; Lee, Ling, Wong, & Poon, 2011; Lee, Sun, Lung, & Chai, 2013; Ling & Poon, 2014; Modro NLR, Modro NR[1], Modro NR[2], & Oliveira, 2009; Soutsos, Tang, & Millard, 2011; Souza, Soriano, & Patino, 2018; Torkaman, Ashori, & Sadr Momtazi, 2014).

The glass fiber reinforced polymer (GFRP) is a composite of glass fiber (reinforcement) and polyester resin (matrix) and addition of the catalyst for fast hardening. Glass fiber represents on average 45% of the GFRP composition, being responsible for the frame and the associated high mechanical resistance. The glass fiber reinforced polymer (GFRP) industry in Brazil has had a great growth, due to its excellent mechanical properties and low density, but it is responsible for the high volume of waste, 13,000 tons. year^{-1} (Orth, Baldin, & Zanotelli, 2012). It has a very low degradability, 300 years for decomposition (Kemerich, Piovesan, Bertoletti, Altmeyer, & HohmVorpagel, 2013). It is estimated that the residue generated by GFRP is 5 to 40% of the total volume produced (Bains & Stokes, 2013). When the recycling of the GFRP residue is done correctly, it has two destinations: landfill or incineration. In both processes a large energy demand is required, mainly for the incineration, since the GFRP residue needs a burning temperature higher than 1000 °C.

The use of synthetic fiber residue in constructive materials, in addition to the sustainable bias, combines its excellent properties with the matrices of materials, making materials with better physical and mechanical properties. The replacement of GFRP by sand in the production of concrete slabs and pavements is feasible in small additions (Correia, Almeida & Figueira, 2011). The use of fiberglass meshes in adobe masonry mortars is

feasible, presenting better shear strength due to seismic shocks (Giamundo, Lignola, Prota, & Manfredi, 2014). The use of GFRP residue in mortars improves the compressive strength, in addition to showing a less fragile behavior, increase the capacity of load absorption, structuring the material (Ribeiro et al., 2011).

No studies were found that replace cementitious matrices with GFRP residue fiber in concrete blocks. However, the partial replacement of the soil matrix by GFRP residue fiber in adobes showed significant improvements related to physical, mechanical and, mainly, thermal properties (Gandia, Gomes, Corrêa, Rodrigues, & Mendes, 2019).

Therefore, the study aimed to produce and investigate the effect of addition of GRFP residue in concrete blocks due to physical, mechanical and thermal properties.

2. Material and Methods

2.1 Materials characterization

2.1.1 Cement, fine gravel, gravel powder and Sand

The binder used is the Portland type CP V-ARI characterized by high strength in the first seven days of the same magnitude of the other binders at twenty-eight days. This performance is due to the finer grinding and the dosing of the clay and limestone in the production of clinker NBR 16697 (Associação Brasileira de Normas Técnicas - ABNT, 2018). The composition of the binder is shown in Table 1.

**Table 1.** Composition of the binder.

Binder	Composition (% by mass)		Standard
	Clinker + plaster	Carbonate material	
CP V –ARI	100-95	0-5	(NBR16697/2018)

Source: Authors (2020).

The aggregates (fine gravel, gravel powder and sand) were characterized by the granulometry NBR NM 248 (Associação Brasileira de Normas Técnicas - ABNT, 2003) and specific mass NBR NM 52 (Associação Brasileira de Normas Técnicas - ABNT, 2009).

The large aggregate (fine gravel) had a mean grain size of 3 to 9 mm. The intermediate aggregate (gravel powder) presented a mean grain size of 2 to 5 mm. The small aggregate (sand) had a mean particle size of 0.04 to 0.3 mm. Figure 1 shows the grain size curves.

Figure 1. Granulometric curve for the aggregates: fine gravel, gravel powder and sand.
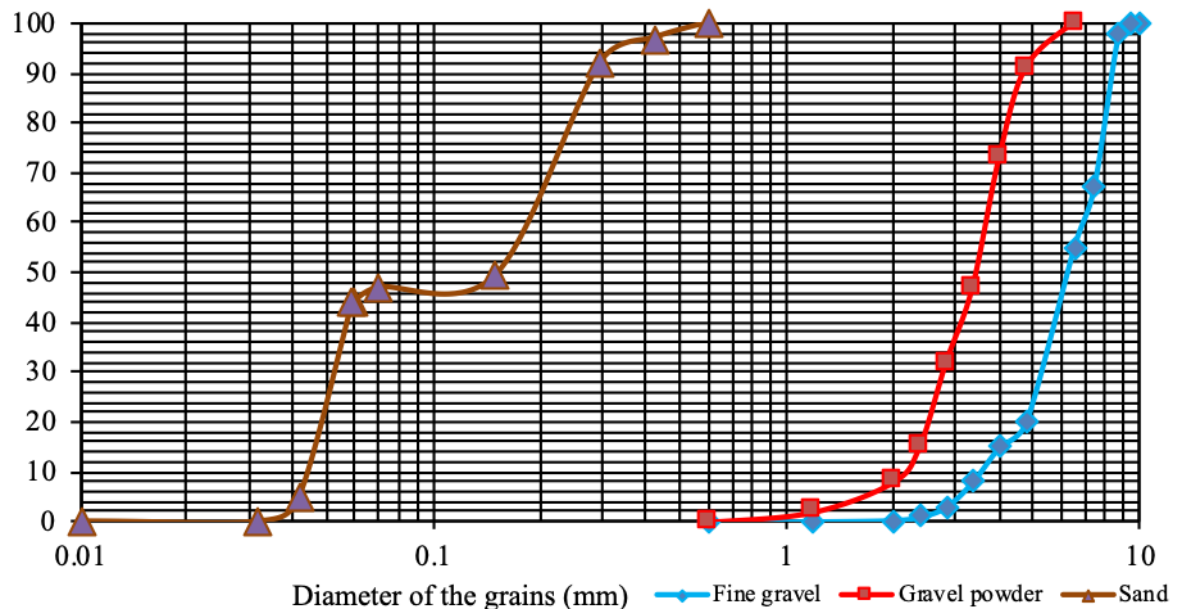
Source: Authors (2020).

The aggregates presented different granulometry intervals, favoring the filling of the mass of the concrete block. Therefore, accommodating the fraction of the components and reducing the voids by packing the particles, allowing greater mechanical resistance and lower water absorption.

The specific mass of the aggregates was obtained in triplicate. The values are presented in Table 2. The fine gravel and the gravel powder presented very similar values. The reason is due to the same mineralogical composition and because the test disregarded the voids between the materials.

Table 2. Specific mass of aggregates.

| Material	Especific mass (g.cm^{-3})	Standard deviation (g.cm^{-3})
Sand	2.43	0.14
Fine gravel	2.67	0.07
Gravel powder	2.64	0.12

Source: Authors (2020).

2.1.2 Glass fiber reinforced polymer (GRFP) waste

The GFRP waste was granted by FIBRASIL, a company that manufactures water boxes and other various materials, generating a high volume of monthly waste with a high cost for logistics to transport until the disposal and with the landfill recycling process.

The GFRP waste is composed of 3 components: resin, glass fiber and catalyst. According to the company, the resin, matrix phase, is unsaturated polyester used manually or by spray. The resin has excellent wettability and impregnation in the glass fibers, the optimum operating temperature being between 20 and 30 °C, some properties of the resin: viscosity 330 to 350 cPs; modulus of elasticity 2.2 and 2.8 GPa in traction and flexion respectively; maximum resistance 40.2 and 84.2 MPa in traction and flexion respectively; density 1.10 g.m^{-3}. The fiberglass originates from two models: blanket of chopped yarns and filaments. The molding is done by hand lay-up and spray-up having excellent mechanical properties, rapid impregnation and uniform dispersion. The catalyst used to accelerate the resin hardening reaction process is methyl ethyl ketone peroxide, represents 5% of mass in the composition of the composite.

In this work, the GFRP waste was processed, triturated and selected. A crusher with a three-phase motor of 7.5 hp was used. The particle size was controlled with an 8.5 mm sieve. From the crushing process, two sub-residues were generated (Figure 2). The "wool" residue was discarded, but separated for future research, using only the residue with the largest volume of glass fibers.

Figure 2. Processing GFRP waste.
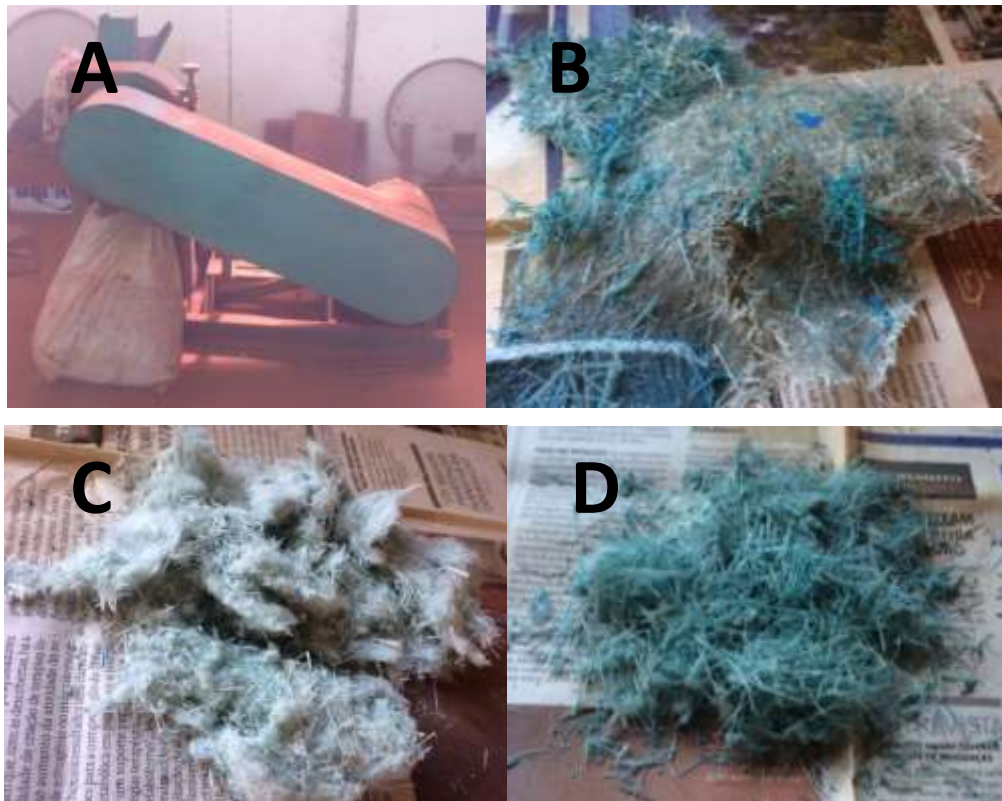
A) GFRP waste. B) Crusher. C) Sub-residue not used ("wool"). D) Sub-residue used.
Source: Authors (2020).

The GFRP residue after processing was analyzed according to aspect ratio, specific mass, chemical composition, and thermogravimetry. The particles after were analyzed with ImageJ software (Figure 3A). Were selected 100 samples of random fibers, finding an average length of 10.507 ± 0.439 mm and an average diameter of 0.04404 ± 0.008 mm. The aspect ratio (L / D) was 238.58. The microstructure of GFRP residue after grinding (Figure 3B) consists of small glass filaments enveloped by resin.

Figure 3. Particles of GFRP waste to medium size analysis and microstructure.
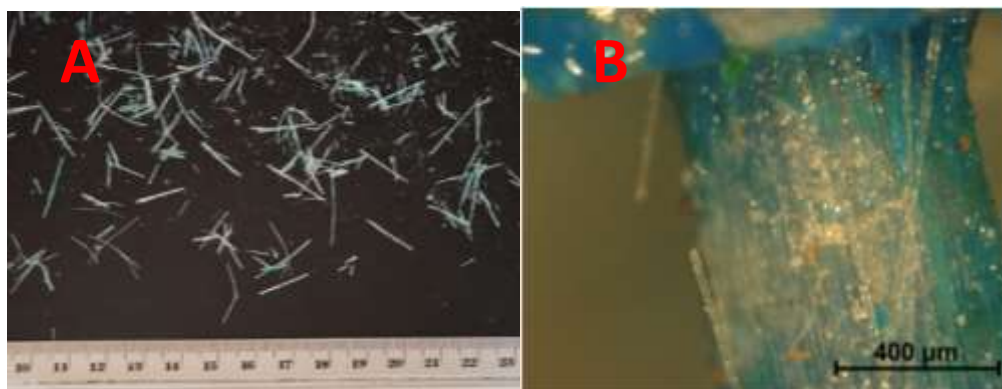
Source: Authors (2020).

The determination of the specific mass of GFRP residue was made in triplicate NBR NM 52 (Associação Brasileira de Normas Técnicas - ABNT, 2009). The value obtained was 1.25-$\pm$ 0.09g cm^{-3}. Ribeiro et al. (2013) found 1.91g cm^{-3}; the specific mass varies depending on the manufacturing and disposal process of each company.

The chemical composition of the residue was found using an X-ray fluorescence spectrometer model S1 Titan LE Serial SMX-1187. The samples were crushed and sifted in a 0.3 mm sieve. Three replicates of the samples were made and the intermediate value (Table 3) was used.

Table 3. Chemical composition of GFRP.

COMPONENT	%
C	65.87
CaO	19.63
SiO2	11.18
Al2O3	2.12
Ti	0.64
Fe	0.25
Cl	0.13
P2O5	0.10
Sr	0.04
Co	0.03
Mn, Zn, Rb, Zr, Cu, Pb e Ni	$\leq$ 0.009

Source: Authors (2020).

Most of the residue is carried by calcium oxide and silicon dioxide. Pinto and Rossi (2009) using X-ray fluorescence spectroscopy showed that the C, Ca, Si and Al elements correspond respectively to 83.73, 7.33, 5.88 and 1.22 of the GFRP waste composition. As a residue, the composition of the GRFP supplied by the manufacturers may vary and may also contain impurities. To determine the composition of the GRFP residue, thermogravimetric analysis ASTM E1131 (American Society for Testing and Materials - ASTM, 2014) was performed (Figure 4). A Shimadzu-DTG 60H analyzer was used. The scans were performed between 25 and 992 °C with a rate of 10 °C min^{-1} under an inert atmosphere of O_2 and flow of 50 mL.min^{-1}. It was done in triplicate and the intermediate value was used. The initial weight was 5.826 mg.

**Figure 4**. GFRP thermogravimetric graph.
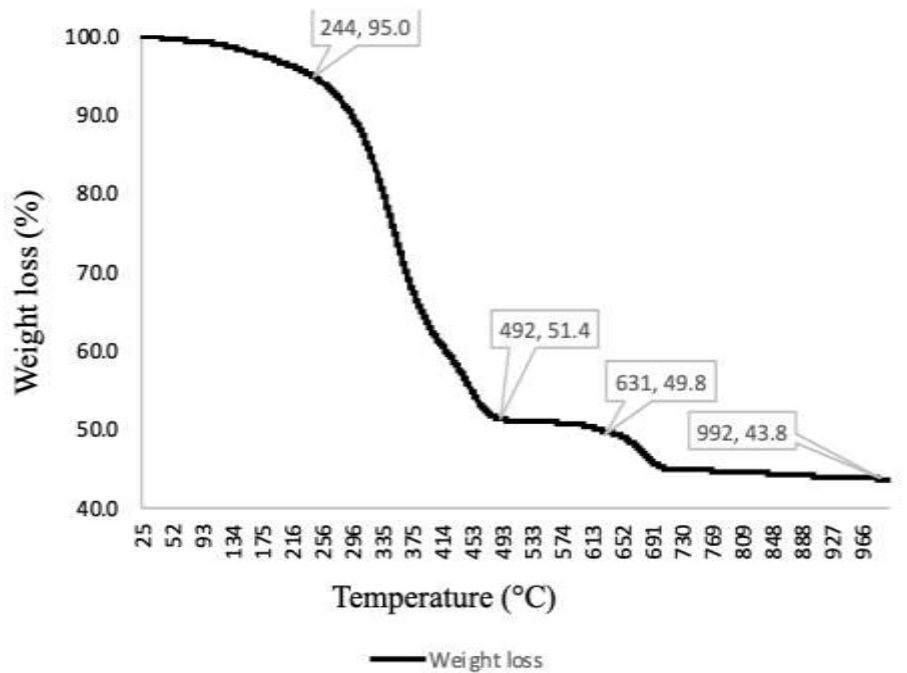
Source: Authors (2020).

There are 4 burn range derived from the composite materials. The first range from 25 to 244 °C refers to catalyst. The second range, 244 at 492 °C, refers to the resin. The third range, 492 at 631°C, refers some impurity or the remaining resin. The fourth range, 631 to 992 °C, refers to glass fiber that has not degraded. Therefore the composition of the GFRP residue was 5% catalyst, 45.2% resin, 6% of a possible impurity and 43.8% of glass fiber.

2.2 Experimental plan and production

Figure 5 shows the components that make up the manufactured blocks. In addition, it can be observed that there was physical, mechanical and thermal variation according to each sample studied.

Figure 5. Graphics experiment.
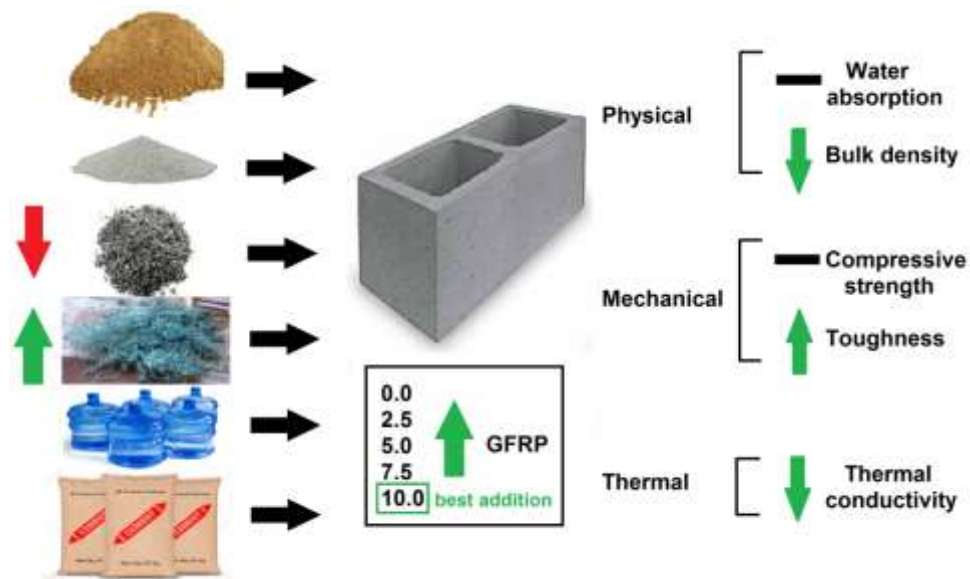
Source: Authors (2020).

Five treatments were produced (Table 4). The day before the production, several samples of the aggregates soil and the GFRP residue were collected to calculate the humidity in the oven for 24 hours at 103 ± 2 °C. The percentages of additions of the materials in each treatment did not vary, with the exception of the GFRP residue and the fine gravel. In Table 4, the materials are presented 0% of water content.

Table 4. Treatments and compositions.

Treatments	GFRP waste (Kg)	Cement (Kg)	Fine gravel (Kg)	Sand (Kg)	Gravel powder (Kg)	Water (kg)
Control	0.0	13.75	37.5	100	62.5	40
GFRP25	1.0	13.75	36.5	100	62.5	40
GFRP50	1.7	13.75	35.8	100	62.5	40
GFRP75	2.8	13.75	34.7	100	62.5	40
GFRP100	3.6	13.75	33.9	100	62.5	40

Source: Authors (2020).

The concrete blocks were manufactured in the same period, with cure period of 28 days. To avoid shrinkage and cracking, two precautions were taken NBR 6136 (Associação Brasileira de Normas Técnicas - ABNT, 2016): the concrete blocks were protected from the

sun, using the ambient temperature for cure; periodic monitored environment with gradual decrease of relative humidity. The Figure 6 shows the blocks before and after the cure process.
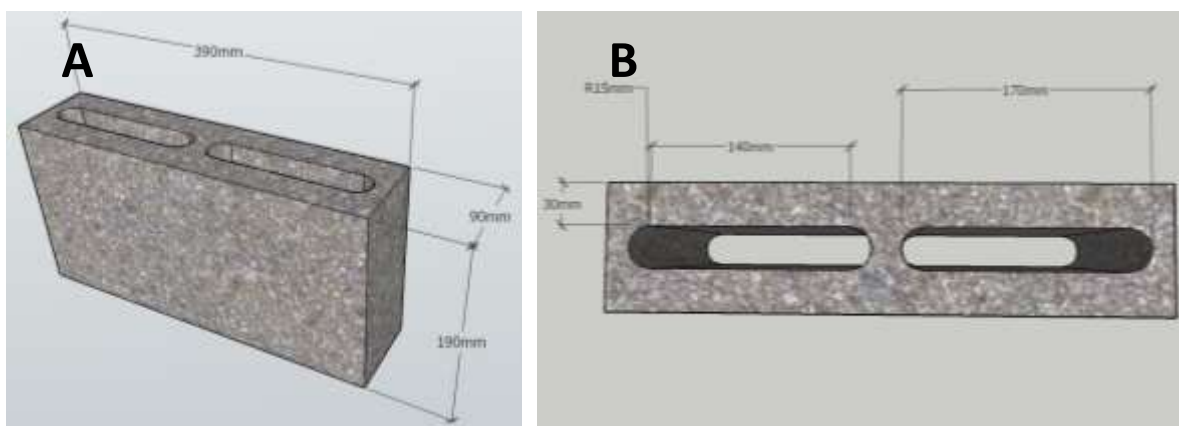
Figure 6. Concrete blocks before and after the cure time.

A)   Blocks after vibration and compression. B) Blocks after 28 days of cure.
Source: Authors (2020).

The size of the shape of vibration and compression of the blocks (width, length and grid) are shown in Figure 7.

**Figure 7.** Dimensions of concrete block.

A) External Isometric view 39x9x19 cm (Length x Height x Width). B) Top View (Holes Details).
Source: Authors (2020).

2.4 Tests

The tests are divided into physical, mechanical, thermal and microstructural. A simplified summary of the tests done to evaluate the concrete blocks was made. The order of execution, the statistics used to evaluate the data, the number of samples and the property to be evaluated in each test can be observed in Figure 8. Subsequently each test is more detailed.

Figure 8. Simplified scheme of the tests in the concrete blocks with GFRP waste.
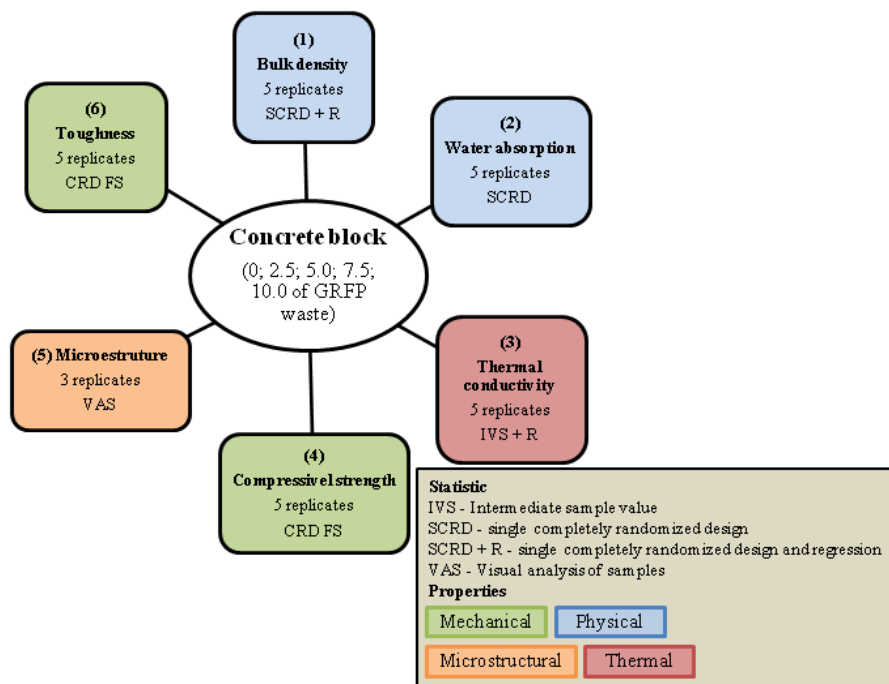
Source: Authors (2020).

2.4.1 Microstructure

Micro structural visualization was done using an SMZ 1500 epi-fluorescence (Nikon) stereoscope microscope. The samples were from the concrete blocks fragments after the compressive strength test to visualize and interpret the interaction between the matrix (agglomerated and aggregate) and the fibers (GFRP residue).

2.4.2 Bulk density

The bulk density test was done according NBR 12118 (Associação Brasileira de Normas Técnicas - ABNT, 2013) with 5 randomly chosen concrete block samples after 28

days of cure period. Twelve measurements were made, 2 for height, 2 for length, 2 for width and 3 pairs of measurements in the directions between the two holes, using a 20 cm digital scaling device and 2 m measuring tape. Figure 9 show the measurements.

Figure 9. Measurements of concrete blocks.

Source: Authors (2020).

The mean of each dimension was calculated by equation (1). The mass was determined using a digital scale in grams. Eq. (1): $d = m\, v^{-1}$, where:

d is the bulk density in $g.cm^{-3}$,

m is the mass in grams (g), and

v is the volume in cubic centimeters (cm^3).

2.4.3 Water absorption

A water absorption test was performed by NBR 12118 (Associação Brasileira de Normas Técnicas - ABNT, 2013). For each treatment, 5 samples of concrete block used after 28 days cure period. The blocks were weighed periodically in an oven until the stabilization of their mass. After the drying process, concrete blocks were weighed (ms). The concrete blocks were submerged in water for 24 hours, after weighed (mu) for calculation of mass difference (water absorption). The water absorption (wa) was calculated by equation (2): wa $(\%) = (mu - ms)\, ms^{-1}\, 100$, where:

wa is the water absorption (%),

mu is the mass of the wet blocks (g), and

ms is the mass of the dried blocks (g).

2.4.4 Thermal analysis

The thermal analysis assay was performed in a chamber composed of MDP (medium density particleboard) of cane bagasse. The chamber has two layers of coatings, styrofoam and a thermal blanket, to isolate the external medium. The lower part contains the heat source (incandescent lamp) connected to a thermostat that maintained the temperature at 47.0 °C. The system had 4 thermocouples: the lamp temperature controller, the ambient temperature, the temperature before entering the sample and the temperature after exiting the sample. The system was connected to an Arduino. To validate the system, the heat output (Figure 10) was verified with an infrared sensor camera, Fluke TI55FT20 / 54 / 7.5, with an accuracy of ± 0.05ºC.

Figure 10. External and upper views of the thermal box and its thermographic images.
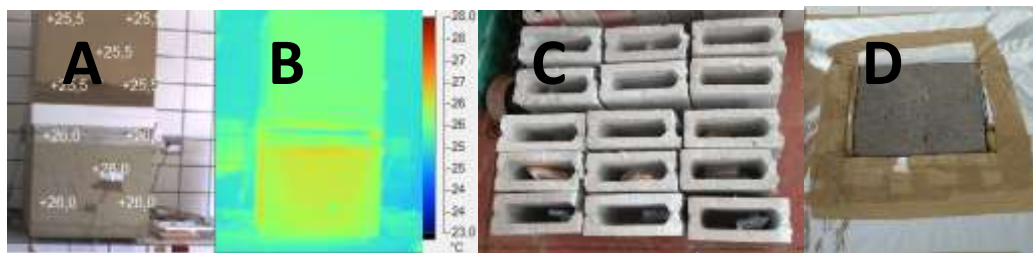
A)   External view of the camera with point temperatures. B) Infrared image of the thermal box and temperature chart. C) Sample cut of concrete blocks. D) Samples positioned and sealed for testing. Source: Authors (2020).

The concrete blocks samples for the thermal assay were cut in a half were cut in half, and positioned for analysis in the smaller position. The samples were 19.5x19x9 cm (height x length x thickness). The temperature difference to stabilization was obtained with a sampling time of 13.33 hours, with 2000 readings of 24 seconds each. Five replicates were made per treatment, and the value of the intermediate sample was used.

To calculate the thermal conductivity (Silva, 2010), the following equation (3) was used:

$K = P E \Delta T^{-1}$ (3), where:

K is the thermal conductivity in $W(m\ ^oC)^{-1}$,

P is the radiation of the incandescent lamp in $W\ m^{-2}$,

E is the thickness of the sample in m, and,

ΔT is the temperature difference to stabilization (ºC).

The radiation of the lamp was determined by a solar radiation meter, Intrutherm model MES-100. Five samples were measured and the mean value was 207.34 W m^{-2}. The temperature variation (ΔT) was determined during the 3.33-hour sampling.

2.4.5 Compressive strength

The compressive strength test was in accordance with NBR 12118 (Associação Brasileira de Normas Técnicas - ABNT, 2013). Before the test, the blocks were regularized at their two ends. The regularization was done with mortar and not exceeding 3 mm each face, according NBR 12118 (Associação Brasileira de Normas Técnicas - ABNT, 2013) (Figure 11A). The test was performed on a Universal mechanical test machine with load capacity of 300 kN, nine samples were tested per treatment. Figure 11B and Figure 11C shows a sample before and after the rupture.

Figure 11. Compression test and preparation of concrete blocks.
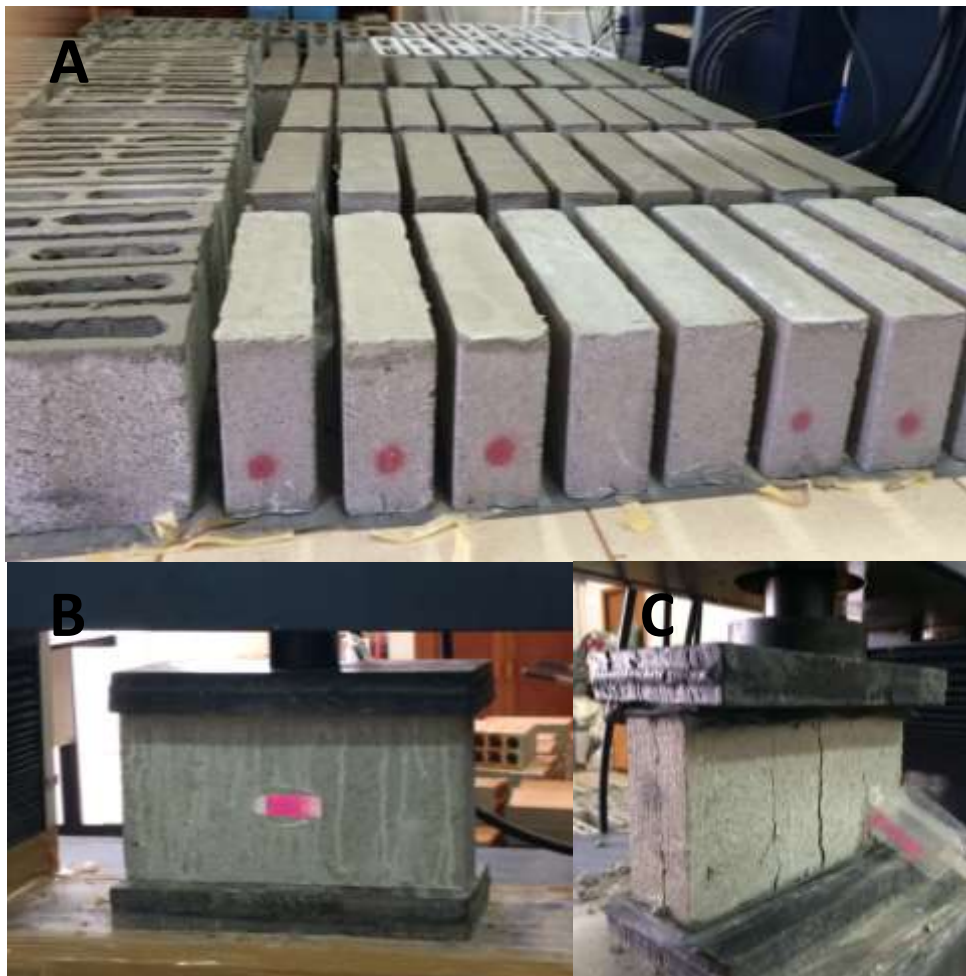
A) Samples of concrete blocks regularized for the compressive strength test. B) Sample before the start of the test. C) Sample after rupture. Source: Authors (2020).

2.4.6 Toughness

In order to verify the loading energy provided by the GFRP waste in the concrete blocks, the toughness test was performed. The Toughness test consisted in using Load-defor curve of the value of the compressive strength analysis of each treatment and each methodology. The area of the curve was calculated just before the point of rupture. The area of the each curve was divided by the area of contact surface of each concrete block sample.

2.5 Statistical analysis

Statistical analysis was partially performed using Sisvar software version 5.6 (Ferreira, 2014). The results of each test: bulk density, water absorption, thermal conductivity, compressive strength and toughness test were statistically analyzed in a single completely randomized design. The Tukey test was used to analyze the significant differences at 5%.

3. Results and Discussion

3.1 Microstructure

The reinforcement of GFRP waste fibers in the concrete blocks was observed in the stereoscope microscope (Figure 12).

Figure 12. Fracture surface of concrete block microstructure.
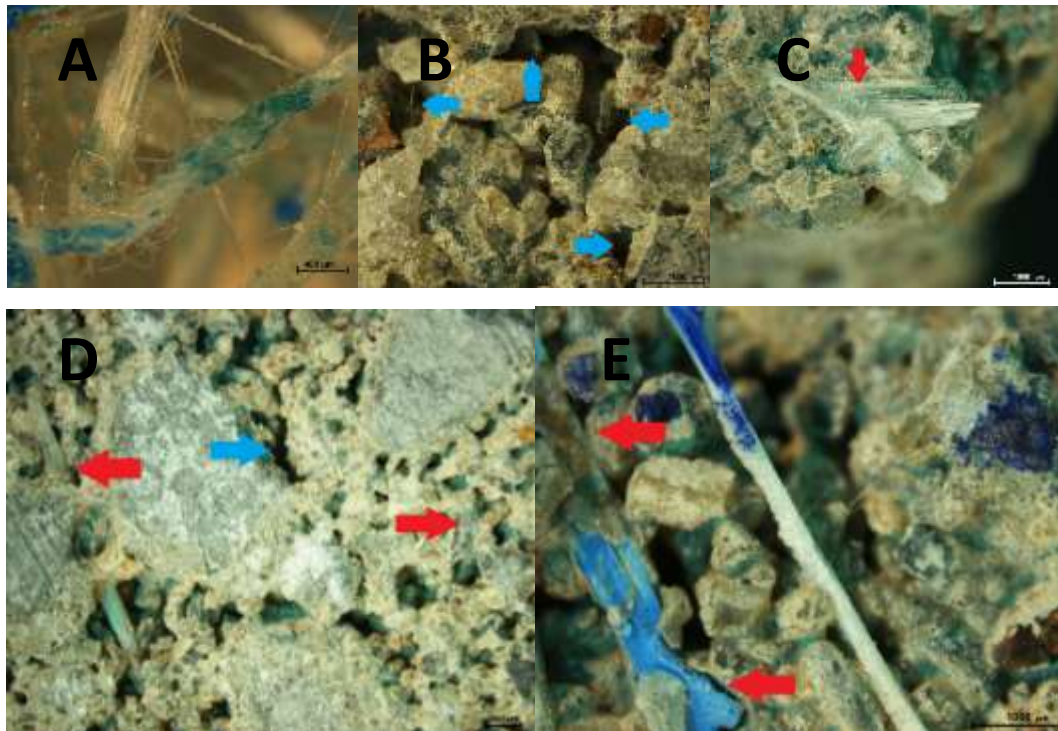
A)   GFRP residue. B) Control treatment. C), D) and E) GFRP100. The blue arrows indicate the presence of pores, the red arrows indicate the cohesion between the GFRP residue and the matrix. Source: Authors (2020).

From the microstructure of the GFRP residue after grinding (Figure 12A), it is possible to observe that the impregnated resin makes the fiber with a more rough appearance, allowing greater adhesion and cohesion between binder/aggregates/residue (matrix-fiber).

The control treatment presented larger and irregular pores, allowing places of greater fragility. Concrete blocks subject to mechanical stresses allow more unpredictable ruptures due to these fragility points. In addition, the heat transfer occurs more rapidly, increasing the thermal conductivity.

The use of the GFRP residue as a fiber makes it possible to fill the matrix in the concrete block. It is possible to observe the interweaving of the binder and aggregates in the GFRP residue, indicating a good cohesion. The GFRP residue acts as a mesh in the matrix of the concrete block, setting and structuring.

3.2 Physical properties of concrete blocks

3.2.1 Bulk density

The bulk density of the concrete blocks decreases with the increase of the GFRP wastes (Figure 13). The concentration of 10% presented a reduction of 0.15 g.cm⁻³ when compared to the control. The GFRP waste (1.25 g.cm^{-3}) presents a much lower density of the binder and aggregates (2.43 – 3.15 g.cm^{-3}), decreasing the bulk density.

Figure 13. Bulk density by the addition of GFRP waste.
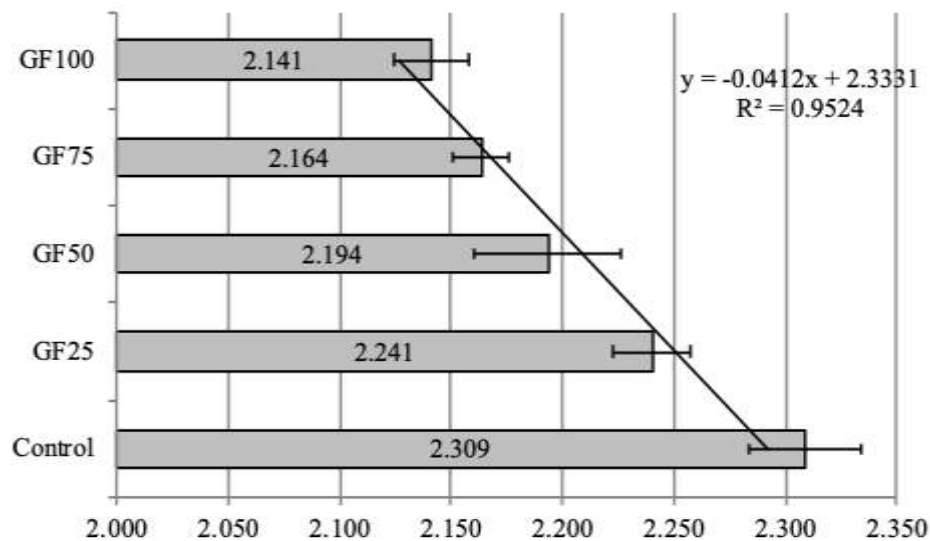
Source: Authors (2020).

The use of GFRP residue at concentrations of 2.5, 5.0, 7.5 and 10% in soil matrix promoted a gradual decrease in bulk density due to lower specific mass of GFRP residue and higher composite porosity promoted by incorporation of GFRP residue at the manufacturing stage (Gandia et al., 2019).

The decrease of the bulk density in materials becomes advantageous for the better workability in the construction and greater efficiency in transport logistics.

The use of river sand and glass aggregates in varying particle sizes in concrete block making showed that glass aggregates reduced concrete block density in 2.3 to 2.1 g.cm^{-3} using river sand and glass aggregates respectively (Yang, Ling, Cui, & Sun, 2019).

The use of fibers in cementitious matrices promotes lower bulk density and greater water absorption through the creation of capillary network and larger number of voids at the

microstructure level. In addition, fibers act as air incorporating agents in the mixing process of composites (Savastano, Warden, & Coutts 2003; Silva, Toledo Filho, Melo Filho, & Fairbairn, 2010).

3.2.2 Water absorption

Figure 14 presents the results for the water absorption of concrete blocks made with the different mixtures. The use of GFRP residue promoted an increase in water absorption. The addition of 2.5% presented the highest value, but all additions are statistically equal.

Figure 14. Water absorption in concrete blocks.
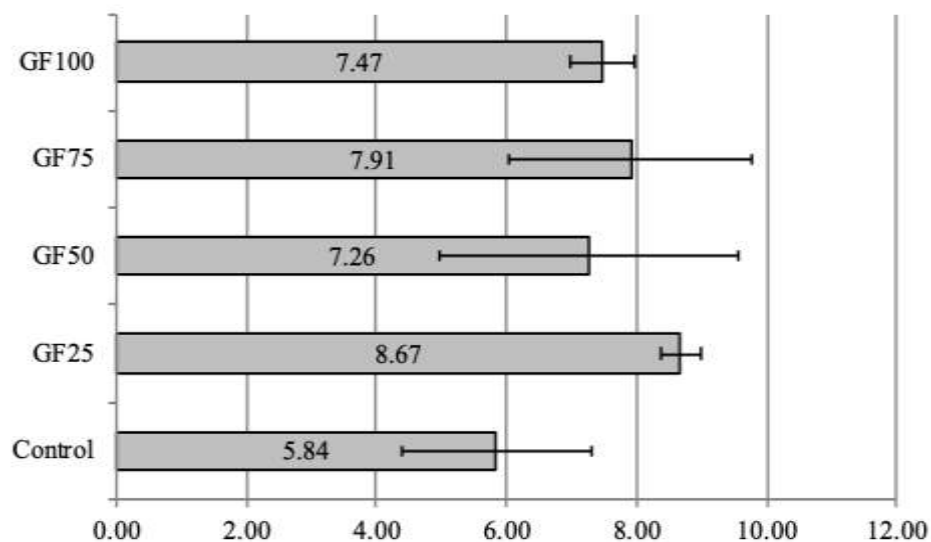
Source: Authors (2020).

According to NBR 6136 (Associação Brasileira de Normas Técnicas - ABNT, 2016) the water absorption in concrete blocks should be less than 10%. Therefore, all treatments are in accordance with the norm.

The use of GFRP residue at concentrations of 2.5, 5.0, 7.5 and 10% in soil matrix promoted a gradual increase in water absorption due to the homogenization of the composite promoting the increase of small pore volume, facilitating the capillarity water entry. However, despite the increase in water absorption, the composite showed lower mass loss, well-defined geometry and stability in contact with water (Gandia et al., 2019).

The use of polymeric waste in 5, 10, 15, 20 and 25% in concrete blocks showed a gradual increase in water absorption, meeting the standard up to 10% of waste (Mattar & Viana, 2012).

3.3 Thermal conductivity

Thermal conductivity decreases with increasing concentrations of GFRP waste. GFRP100 presented the lowest value in comparison to the other treatments (Figure 15).

Figure 15. Mean values for thermal conductivity in W.(m °C)$^{-1}$.
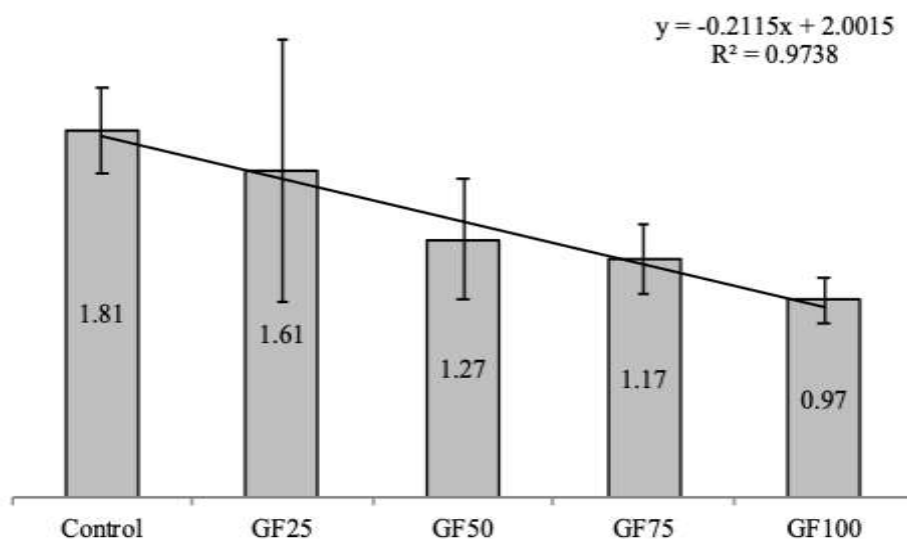
Source: Authors (2020).

Yang et al. (2019) obtained similar thermal conductivity values in traditional concrete blocks of approximately 2.0 W (m.°C)$^{-1}$. The use of river sand and glass aggregates in varying particle sizes in concrete block making showed that glass aggregates in addition to reducing concrete block density also significantly reduced thermal conductivity from approximately 2.0 to 0.8 W.(m.°C)$^{-1}$, respectively with river sand and glass aggregates (Yang et al., 2019).

Analyzing the properties of concrete floor block using marble residue and perlite aggregates, Alyousef et al. (2019), observed the decrease of thermal conductivity up to 56% correlated with the decrease of apparent density of the material.

Gandia et al. (2019) using GFRP residue in adobe at concentrations of 0 to 10% by mass found a 30% reduction in thermal conductivity when 10% GFRP residue was added.

The authors state that increased porosity promoted by GFRP residue and GFRP residue itself, which is an insulating material, contribute to the decrease in thermal conductivity. In addition, the bulk density ratio may be directly related to thermal conductivity.

The lower thermal conductivity is related to lower energy expenditure after the construction (Millogo, Aubert, Séré, Fabbri, & Morel, 2016). Concrete block is already considered a material with a lower energy demand compared to ceramic materials (Gandia et al., 2018). One of the reasons that the concrete block presents less embodied energy is the non-burning of the material. The fact that the concrete block with GFRP residue presents a relatively low thermal conductivity will accentuate an energy reduction after construction. This reduction causes less energy to be expended to heat or cool the environment due to the lower exchange of radiation with the external environment provided by the low thermal conductivity of the material.

The use of the GFRP residue in concrete block improves its thermal properties, reducing the transfer of heat and presenting better thermal comfort. It can be stated that the GFRP waste is a thermal insulator. The lower stabilization temperature reduction can be explained by the higher number of pores due to the higher concentration of GFRP residue. This is also associated with the bulk density, and it is possible to make an association of the decrease of the density of the concrete block according to the increase of the GFRP residue related to the increase of the thermal inertia.

3.4 Compressive strength

The use of GFRP residue decreases the compressive strength of the concrete blocks. However the treatments present statistically equal values. Figure 16 shows that increasing the GFRP residue concentration in the concrete blocks promoted more homogeneous materials, considerably reducing the standard deviation in additions above 5%.

Figure 16. Mean values and standard deviations of the compressive strength (MPa).
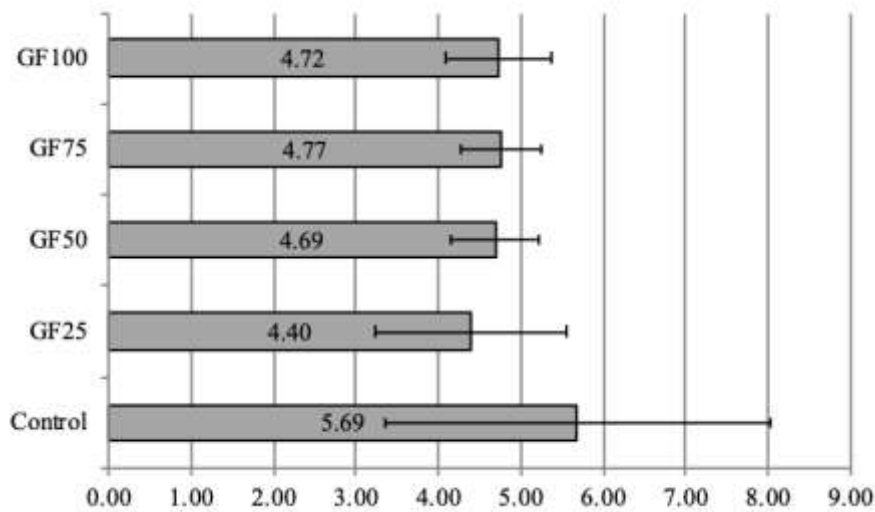
Source: Authors (2020).

The possible reason for more standardized concrete blocks is due to three factors: cohesion of GFRP residue in the matrix due to the roughness promoted by the polymer in the fiberglass; structuring of the concrete block promoted by GFRP residue, acting as a mesh in the composite and filling the empty spaces in the cementitious matrix, increasing the porosity of the concrete blocks, but with less and well distributed pores. The statements are noted in the microstructure test (Figure 12).

The NBR 6136 (Associação Brasileira de Normas Técnicas - ABNT, 2016) determines that sealing concrete blocks have values above 3 MPa, therefore all treatments were accepted by the standard. All average values and deviations are above 3 MPa.

The use of GFRP residue at concentrations of 2.5, 5.0, 7.5 and 10% in soil matrix promoted a 49% increase in the addition of 10% in relation to the non-addition (Gandia et al., 2019). The use of plastic waste between 5 and 25% in concrete blocks showed that 5% obtained an average value of 3.71 MPa, 10% was below 3 Mpa and above 10% the concrete blocks are dismantled after molding (Mattar & Viana, 2012). River sand and glass aggregates in varying particle sizes in concrete block making showed that glass aggregates reduced concrete block compressive strength by 20% (Yang et al., 2019).

GFRP residue has good mechanical properties, but its use in cementitious matrices is limited. The ideal concentration of GFRP residue is related to the aspect ratio of the residue and its cohesion power in the cementitious matrix.

Consoli, Montardo, Donato, and Prietto (2004) examining the effect of glass fiber addition on cemented soils, showed a significant improvement in the fragile behavior of the

soil without the addition of glass fibers. This decrease in soil fragility influences both the increase in compressive strength and the increase in energy absorption due to the load, presenting a non-brittle rupture due to the greater deformation.

The addition of the GFRP residue in concrete blocks besides does not significantly influence resistance to rupture, increases the load absorption capacity, predicting the collapse. In Figure 17 is observed a higher load absorption and higher deformation according to the addition of GFRP residue.

Figure 17. Load-strain curves of concrete blocks, obtained from the intermediate sample by treatment.
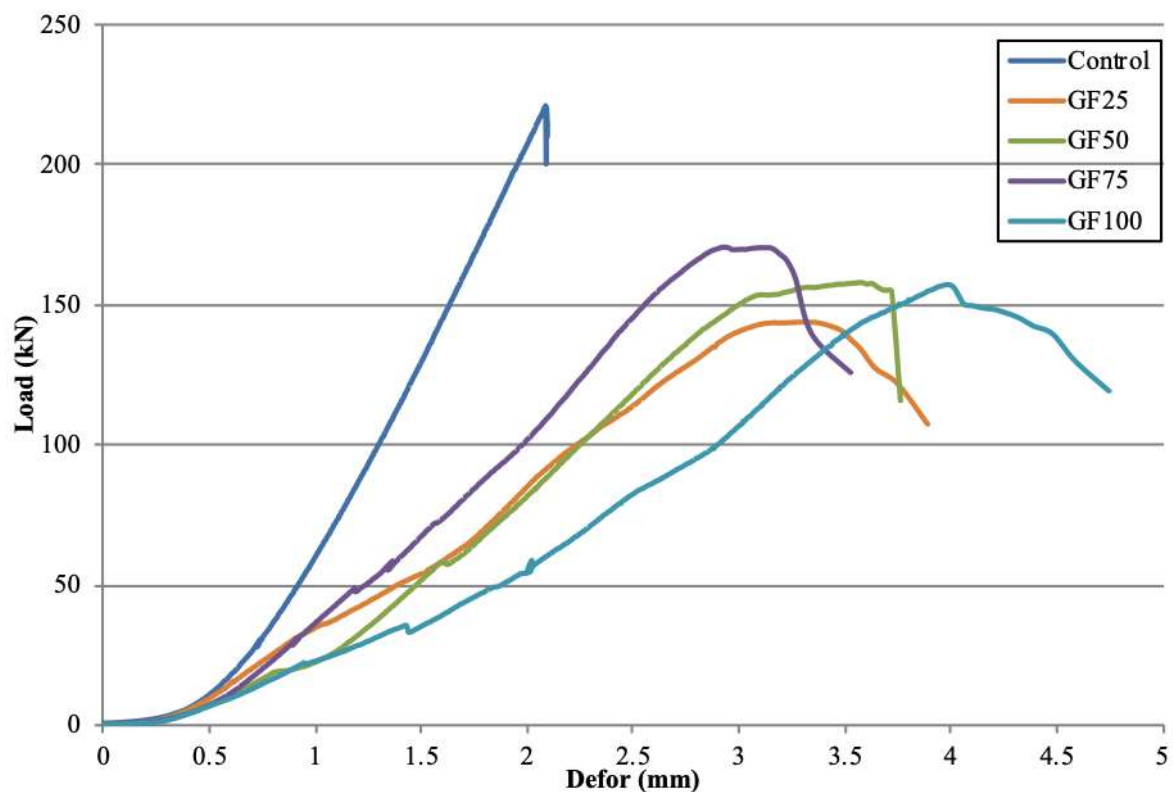
Source: Authors (2020).

In Figure 18, it also noted is the increase in deformation of the material as a function of the greater addition of GFRP residue. The increase in the Load-strain curves area formed at the time of the rupture of material is proportional to the increase in the tenacity of the material. Therefore, the toughness is proportional to the increase in the concentration of GFRP residue.

Figure 18. Average toughness obtained from the compression test (MPa).
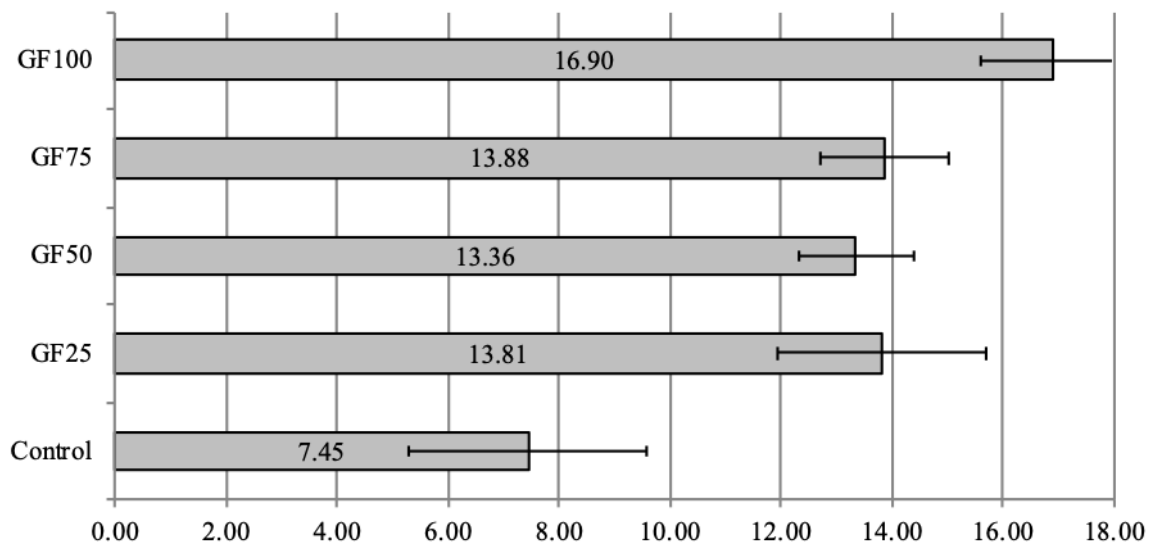
Source: Authors (2020).

The GFRP residue has good mechanical properties and excellent cohesion between the cementitious matrixes. The structuring of the concrete blocks coming from the residue allows that the load applied to the concrete blocks will be absorbed by the fibers of the residue that will absorb this compressive energy, therefore higher deformation before the collapse. The capacity of higher absorption of the compressive energy is also associated with the greater fixation of the matrix with the fibers of the residue. The ductility characteristic promoted by the fibers of the residue gives a less abrupt rupture. This characteristic in the constructive context is more favorable, aiming at structural safety.

3.5 Synthesis of test results

For a better understanding of the tests, a table was created summarizing all the results. Table 5 presents all the results regarding the tests performed in this work. The control treatment is the reference value to the others. The other treatments are directly related to control treatment (0% of GFRP) by increase and decrease.

Table 5. Synthesis of the tests (%).

Tests	Treatments								
	Control	GFRP25		GFRP50		GFRP75		GFRP100	
Bulk density	0.00	-	2.94	-	4.98	-	6.28	-	7.28
Water absorption	0.00	+	48.46	+	24.32	+	35.45	+	27.91
Thermal conductivity	0.00	-	11.05	-	29.83	-	35.36	-	46.41
Compressive strength	0.00	-	22.67	-	17.57	-	16.17	-	17.05
Toughness	0.00	+	85.37	+	79.33	+	86.31	+	126.85

All values are in consideration of the control (C) treatment and in %. The + and - signs refer to the increase or decrease in the values of the other treatments in relation to the control treatment.
Source: Authors (2020).

The results indicated a gradual trend of increase and decrease by the addition of GFRP waste in the concrete block. A gradual decrease in bulk density and thermal conductivity were observed. The decrease of these values is favorable for the improvement of the physical and thermal properties of the concrete block with GFRP. The gradual increase was evidenced in the toughness test. The increase of these values provides improvement in the mechanical properties of the concrete block. The compressive strength and water absorption analyzes, although presenting differences in the results, showed no statistical difference between the use and non-use of GFRP residue, besides the result of all treatments meeting the standards.

4. Conclusions

The results of this work demonstrated that it is possible to improve the physical, mechanical and thermal properties of the concrete blocks using the glass fiber reinforced polymer waste (GFRP). The use of the GFRP waste reduced bulk density. The addition of the GFRP waste also promoted a decrease in the thermal conductivity of the concrete blocks, consequently, improving its thermal comfort in a house. There was a small decrease in the compressive strength of the concrete block, but statistically equal however, the toughness increased more than twice, stating the energy absorption power of the residue. The concentration of 10% GFRP waste showed the best results. The GFRP waste presented good cohesion to the matrix (binder and aggregates), allowing greater structuring and reinforcement, resulting in more structured concrete block. The lower mass of the concrete block promotes better workability and easy transportation. The waste in question has a high

decomposition period and large-scale production, but contains valuable constructive properties. Therefore, in this work, an alternative way to introduce a residue in composite construction materials was presented.

As a proposal to continue the studies carried out and exposed here, in order to deepen the feasibility of using reinforced polymer waste in the manufacture of concrete blocks, studies using new dosages are suggested, aiming to improve the line with the optimum content replacement. In addition, studies of accelerated aging of fibers in a concrete block, to analyze their degradation time, are also suggested.

References

Algin H. M., & Turgut P. (2008). Cotton and limestone powder wastes as brick material. *Construction and Building Materials*, 22(6), 1074–1080. doi:10.1016/j.conbu ildmat.2007.03.006

Alyousef R., Benjeddou O., Soussi C., Khadimallah M. A., & Jedidi M. (2019). Experimental Study of New Insulation Lightweight Concrete Block Floor Based on Perlite Aggregate, Natural Sand, and Sand Obtained from Marble Waste. *Advances in Materials Science and Engineering*, 2019, 14. doi:10.1155/2019/8160461

Ascione L., De Felice G., De Santis S. (2015). A qualification method for externally bonded Fibre Reinforced Cementitious Matrix (FRCM) strengthening systems. *Composites Part B: Engineering*, 78, 497–506. doi:10.1016/j.compositesb.2015.03.079

ABNT - Associação Brasileira de Normas Técnicas (2018). *NBR 16697*. Portland cement - Requirements. Rio de Janeiro, ABNT, 12 p.

ABNT - Associação Brasileira de Normas Técnicas (2003). *NBR NM 248*. Aggregates - Sieve analysis of fine and coarse aggregates. Rio de Janeiro, ABNT, 6 p.

ABNT - Associação Brasileira de Normas Técnicas (2009). *NBR NM 52*. Fine aggregate - Determination of the bulk specific gravity and apparent specific gravity. Rio de Janeiro, ABNT, 6 p.

ABNT - Associação Brasileira de Normas Técnicas (2013). *NBR 12118*. Hollow concrete blocks for concrete masonry — Test methods, Rio de Janeiro, ABNT, 14 p.

ABNT - Associação Brasileira de Normas Técnicas (2016). *NBR 6136*. Hollow concrete blocks for concrete masonry — Requirements, Rio de Janeiro, ABNT, 10 p.

ASTM. (2014). *ASTM E1131*. Standard Test Method for Compositional Analysis by Thermogravimetry. ASTM International, West Conshohocken, PA.

Bains M., & Stokes E. (2013). Developing a Resource Efficiency Action Plan for the Composites 523 Sector. URS & Netcomposites.

Bilodeau A., Kodur V. K. R., & Hoff G. C. (2004). Optimization of the type and amount of polypropylene fibres for preventing the spalling of lightweight concrete subjected to hydrocarbon fire. *Cement and Concrete Composites*, 26(2), 163–174. doi:10.1016/S0958-9465(03)00085-4

Brandt A. M. (2008). Fibre reinforced cement-based (FRC) composites after over 40 years of development in building and civil engineering. *Composite Structures*, 86(1–3), 3–9. doi:10.1016/j.compstruct.2008.03.006

Callejas I. J. A., Durante L. C., & Oliveira A. S. (2017). Construction and demolition conductivity of recycled Thermal resistance and waste (RCDW) concrete blocks. *Civil Engineering*, 70(2), 167–173. doi:10.1590/0370-44672015700048

Carozzi F. G., Milani G., & Poggi C. (2014). Mechanical properties and numerical modeling of Fabric Reinforced Cementitious Matrix (FRCM) systems for strengthening of masonry structures. *Composite Structures*, 107, 711–725. doi:10.1016/j.compstruct.2013.08.026

Chen Z., Li J. S., Poon C. S. (2018). Combined use of sewage sludge ash and recycled glass cullet for the production of concrete blocks. *Journal of Cleaner Production*, 171, 1447–1459. doi:10.1016/j.jclepro.2017.10.140

Choi Y., Moon D., Chung J., & Cho S. (2005). Effects of waste PET bottles aggregate on the

properties of concrete. *Cement and Concrete Research*, 35, 776–781. doi:10.1016/j.cemconres.2004.05.014

Consoli N. C., Montardo J. P., Donato M., & Prietto P. D. M. (2004). Effect of material properties on the behaviour of sand?cement?fibre composites. *Ground Improvement*, 8(2), 77–90. doi:10.1680/grim.8.2.77.36370

Correia J. R., Almeida N. M., & Figueira J. R. (2011). Recycling of FRP composites: Reusing fine GFRP waste in concrete mixtures. *Journal of Cleaner Production*, 19(15), 1745–1753. doi:0.1016/j.jclepro.2011.05.018

Dimitrioglou N., Tsakiridis P. E., Katsiotis N. S., Katsiotis M. S., Perdikis P., & Beazi M. (2016). Production and Characterization of Concrete Paving Blocks Containing Ferronickel Slag as a Substitute for Aggregates. *Waste and Biomass Valorization*, 7(4), 941–951. doi:0.1007/s12649-015-9465-1

Fajardo V. M. S., Torres M. E., & Moreno A.J. (2015). Hydraulic and hygrothermal properties of lightweight concrete blocks with basaltic lapilli as aggregate. *Construction and Building Materials*, 94, 398–407. doi:10.1016/j.conbuildmat.2015.07.020

Ferreira D. F. (2014). Sisvar: a Guide for its Bootstrap procedures in multiple comparisons. *Ciência e Agrotecnologia*, 38(2), 109–112. doi: 10.1590/s1413-70542014000200001

Gandia R. M., Campos A. T., Corrêa A. A. R., & Gomes F. C. (2018). Energy costs comparison of masonry made from different materials. *Theoretical and Applied Engineering*, 2(1), 1–8. Retrieved from http://www.taaeufla.deg.ufla.br/index .php/TAAE/issue/view/5/R1023

Gandia R. M., Gomes F. C., Corrêa A. A. R., Rodrigues M. C., & Mendes R. F. (2019). Physical, mechanical and thermal behavior of adobe stabilized with glass fiber reinforced polymer waste. *Construction and Building Materials*, 222, 168–182. doi:10.1016/j.conbuildmat.2019.06.107

Giamundo V., Lignola G. P., Prota A., Manfredi G. (2014). Nonlinear analyses of adobe

masonry walls reinforced with fiberglass mesh. *Polymers*, 6(2), 464–478. doi:10.3390/polym6020464

Kanchanapiya P., Methacanon P., & Tantisattayakul T. (2018). Resources , Conservation & Recycling Techno-economic analysis of light weight concrete block development from polyisocyanurate foam waste. *Resources, Conservation & Recycling*, 138(December 2017), 313–325. doi:10.1016/j.resconrec.2018.07.027

Kemerich P. D. C., Piovesan M., Bertoletti L. L., Altmeyer S., & HohmVorpagel T. (2013). Glass fiber: characterization, disposal and environmental impact generated. *Revista Eletrônica Em Gestão, Educação e Tecnologia Ambiental*, 10(10), 2112–2121. doi:10.5902/223611707590

Konsta-Gdoutos M. S., Metaxa Z. S., Shah S. P. (2010). Highly dispersed carbon nanotube reinforced cement based materials. *Cement and Concrete Research*, 40(7), 1052–1059. doi:10.1016/j.cemconres.2010.02.015

Kus H., Özkan E., Göcer Ö., & Edis E. (2013). Hot box measurements of pumice aggregate concrete hollow block walls. *Construction and Building Materials*, 38, 837–845. doi:10.1016/j.conbuildmat.2012.09.053

Lee G., Ling T., Wong Y., & Poon C. (2011). Effects of crushed glass cullet sizes , casting methods and pozzolanic materials on ASR of concrete blocks. *Construction and Building Materials*, 25(5), 2611–2618. doi:10.1016/j.conbuildmat.2010.12.008

Lee G., Sun C., Lung Y., & Chai T. (2013). Effects of recycled fine glass aggregates on the properties of dry – mixed concrete blocks. *Construction and Building Materials*, 38, 638–643. DOI: 10.1016/j.conbuildmat.2012.09.017

Ling T., & Poon C. (2014). Use of recycled CRT funnel glass as fi ne aggregate in dry-mixed concrete paving blocks. *Journal of Cleaner Production*, 68, 209–215. doi:10.1016/j.jclepro.2013.12.084

Mattar D. C., & Viana E. (2012). Utilização De Resíduos Poliméricos Da Indústria De

Reciclagem De Plástico Em Blocos De Concreto. *Revista Eletrônica Em Gestão, Educação e Tecnologia Ambiental*, 8(8), 1722–1733. doi:10.5902/223611706471

Millogo Y., Aubert J. E., Séré A. D., Fabbri A., Morel J. C. (2016). Earth blocks stabilized by cow-dung. *Materials and Structures*, 49(11), 4583–4594. doi:10.1617/s11527-016-0808-6

Modro N. L. R., Modro N.[1], Modro N.[2], & Oliveira A. P. (2009). Evaluation of concrete made of Portland cement containing PET wastes. *Revista Matéria*, 14(1), 725–736.

Orth C. M., Baldin N., Zanotelli C. T. (2012). Impacts of the manufacturing process using fiberglass reinforced plastic composite on the environment and occupational health: the automotive industry case. *Revista Produção Online*, 12(2), 537–556. doi:10.14488/1676-1901.v12i2.943

Pinto K. N. C., & Rossi J. L. (2009). *Reciclagem de resíduos de materiais compósitos de matriz polimérica: poliéster insaturado reforçado com fibras de vidro*. Universidade de São Paulo, São Paulo.

Ribeiro M. C. S., Fiúza A., Castro A. C. M., Silva F. G., Dinis M. L., Meixedo J. P., & Alvim M. R. (2013). Mix design process of polyester polymer mortars modified with recycled GFRP waste materials. *Composite Structures*, 105, 300–310. doi:10.1016/j.compstruct.2013.05.023

Ribeiro M. C. S., Meixedo J. P., Fiúza A., Dinis M. L., Castro A. C. M., Silva F. J. G. ... Alvim M. R. (2011). Mechanical Behaviour Analysis of Polyester Polymer Mortars Modified with Recycled GFRP Waste Materials. *World Academy of Science, Engineering and Technology*, 5, 3–27. doi:10.5281/zenodo.1058061

Savastano H. J., Warden P. G., & Coutts R. S. P. (2003). Mechanically pulped sisal as reinforcement in cementitious matrices. *Cement & Concrete Composites*, 25, 311–319.

Shuh-Huei L., Shah S. P., Zongjin L., & Toshio M. (1993). Micromechanical analysis of multiple fracture and evaluation of debonding behavior for fiber-reinforced composites. I*nternational Journal of Solids and Structures*, 30(11), 1429–1459. doi:10.1016/0020-7683(93)90070-N

Silva A. R. (2010). *Estudo térmico e de materiais de um bloco para construção de casas populares, confeccionado a partir de um compósito a base de gesso, EPS e raspa de pneu.* Universidade Federal do Rio Grande do Norte, Natal.

Silva F. A., Toledo Filho R. D., Melo Filho J. A., & Fairbairn E. M. R. (2010). Physical and mechanical properties of durable sisal fiber-cement composites. *Construction and Building Materials*, 24(5), 777–785. doi:10.1016/j.conbuildmat.2009.10.030

Soroushian P., & Bayasi Z. (1991). Strength and ductility of steel fibre reinforced concrete under bearing pressure. *Magazine of Concrete Research*, 43(157), 243–248.

Soutsos M. N., Tang K., & Millard S. G. (2011). Concrete building blocks made with recycled demolition aggregate. *Construction and Building Materials*, 25(2), 726–735. doi:10.1016/j.conbuildmat.2010.07.014

Souza M. F., Soriano J., & Patino M. T. O. (2018). Compressive strength and economic viability of concrete blocks with ceramic brick residues. *Revista Matéria*, 23(3), 1–11. doi:10.1590/S1517-707620180003.0537

Swamy R. N. (1975). Fibre Reinforced Cement Based Composites Fibre Reinforcement of Cement and Concrete. *Materials and Structures*, 8(3), 235–254. Retrieved from https://link.springer.com/content/pdf/10.1007%2FBF02475172.pdf

Torkaman J., Ashori A., & Momtazi A. S. (2014). Using wood fiber waste, rice husk ash, and limestone powder waste as cement replacement materials for lightweight concrete blocks. *Construction and Building Materials*, 50, 432–436. doi:10.1016/j.conbuildmat.2013.09.044

Udawattha C., & Halwatura R. (2018). Advances in Building Energy Research Thermal performance and structural cooling analysis of brick , cement block , and mud concrete block. *Advances in Building Energy Research*, 12(2), 150–163. doi:10.1080/17512549.2016.1257438

Xu T., Chen Q., Zhang Z., Gao X., & Huang G. (2016). Investigation on the properties of a

new type of concrete blocks incorporated with PEG/SiO2 composite phase change material. *Building and Environment*, 104, 172–177. doi:10.1016/j.buildenv.2016.05.003

Yang S., Ling T., Cui H., & Sun C. (2019). Influence of particle size of glass aggregates on the high temperature properties of dry-mix concrete blocks. *Construction and Building Materials*, 209, 522–531. doi:0.1016/j.conbuildmat.2019.03.131

Zaetang Y., Sata V., Wongsa A., & Chindaprasirt P. (2016). Properties of pervious concrete containing recycled concrete block aggregate and recycled concrete aggregate. *Construction and Building Materials*, 111, 15–21. doi:10.1016/j.conbuildmat.2016.02.060

Zhu L., Dai J., Bai G., & Zhang F. (2015). Study on thermal properties of recycled aggregate concrete and recycled concrete blocks. *Construction and Building Materials*, 94, 620–628. doi:10.1016/j.conbuildmat.2015.07.058

Percentage of contribution of each author in the manuscript

Jaqueline Damiany Portela – 50%

Rômulo Marçal Gandia – 15%

Bárbara Lemes Outeiro Araújo – 10%

Rodrigo Allan Pereira – 10%

Francisco Carlos Gomes – 15%